RESEARCH

Transplantation of miR-145a-5p modified M2 type microglia promotes the tissue repair of spinal cord injury in mice

Penghui Li[1,2†], Junlong Zhao[2†], Yangguang Ma[1], Liang Wang[2], Shiqian Liang[2], Fan Fan[2], Tiaoxia Wei[2], Lei Feng[2], Xueyu Hu[1], Yiyang Hu[2*], Zhe Wang[1*] and Hongyan Qin[2*]

Abstract

Background The traumatic spinal cord injury (SCI) can cause immediate multi-faceted function loss or paralysis. Microglia, as one of tissue resident macrophages, has been reported to play a critical role in regulating inflammation response during SCI processes. And transplantation with M2 microglia into SCI mice promotes recovery of motor function. However, the M2 microglia can be easily re-educated and changed their phenotype due to the stimuli of tissue microenvironment. This study aimed to find a way to maintain the function of M2 microglia, which could exert an anti-inflammatory and pro-repair role, and further promote the repair of spinal cord injury.

Methods To establish a standard murine spinal cord clip compression model using Dumont tying forceps. Using FACS, to sort microglia from C57BL/6 mice or CX3CR1^{GFP} mice, and further culture them in vitro with different macrophage polarized medium. Also, to isolate primary microglia using density gradient centrifugation with the neonatal mice. To transfect miR-145a-5p into M2 microglia by Lipofectamine2000, and inject miR-145a-5p modified M2 microglia into the lesion sites of spinal cord for cell transplanted therapy. To evaluate the recovery of motor function in SCI mice through behavior analysis, immunofluorescence or histochemistry staining, Western blot and qRT-PCR detection. Application of reporter assay and molecular biology experiments to reveal the mechanism of miR-145a-5p modified M2 microglia therapy on SCI mice.

Results With in vitro experiments, we found that miR-145a-5p was highly expressed in M2 microglia, and miR-145a-5p overexpression could suppress M1 while promote M2 microglia polarization. And then delivery of miR-145a-5p overexpressed M2 microglia into the injured spinal cord area significantly accelerated locomotive recovery as well as prevented glia scar formation and neuron damage in mice, which was even better than M2 microglia

---

†Penghui Li and Junlong Zhao contributed equally to this work.

*Correspondence:
Yiyang Hu
yiyanghu2006@hotmail.com
Zhe Wang
wangzhe@fmmu.edu.cn
Hongyan Qin
hyqin@fmmu.edu.cn
Full list of author information is available at the end of the article

transplantation. Further mechanisms showed that overexpressed miR-145a-5p in microglia inhibited the inflammatory response and maintained M2 macrophage phenotype by targeting TLR4/NF-κB signaling.

Conclusions These findings indicate that transplantation of miR-145a-5p modified M2 microglia has more therapeutic potential for SCI than M2 microglia transplantation from epigenetic perspective.

Keywords miR-145a-5p, M2 microglia, Neuroinflammation, Spinal cord injury

Graphical Abstract
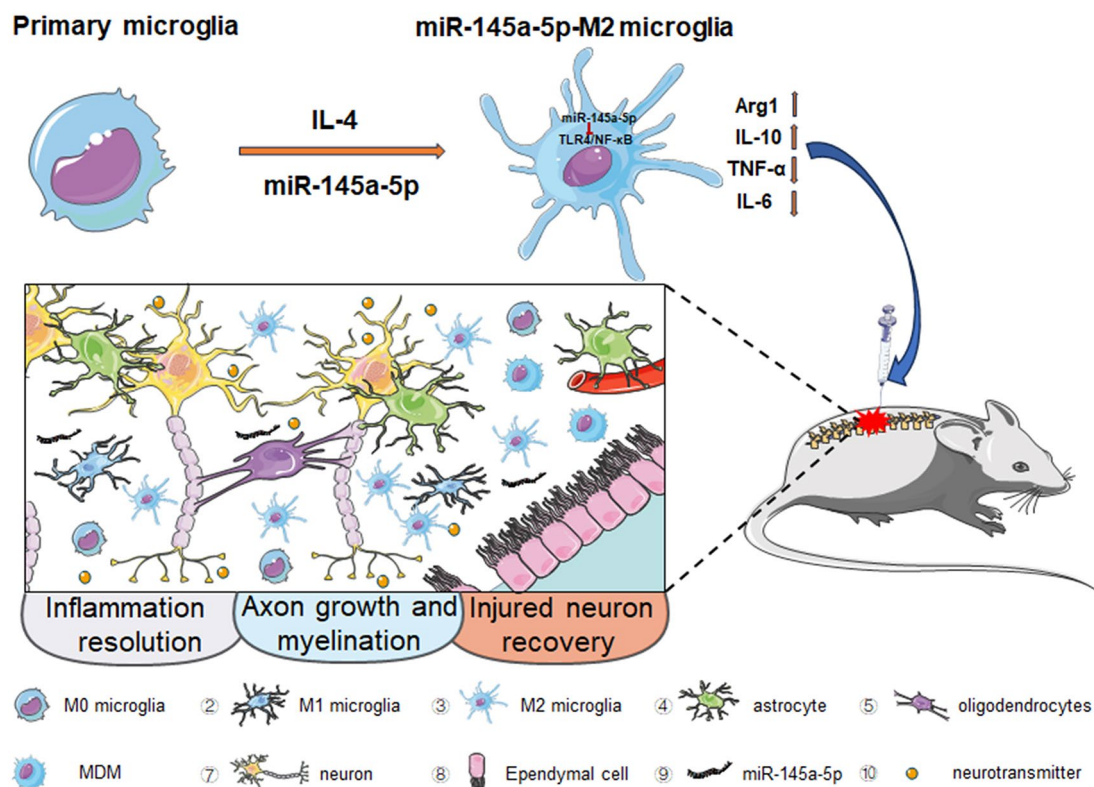
Introduction

Traumatic spinal cord injury is a common neurologic insult worldwide that results in the loss of sensation, motor, and autonomic function. The SCI has been prevalence over the past 30 years, and the incidence rate ranges from 236 to 1298 patients per million in different countries [1]. Although the surgical decompensation is the most effective treatment till now, the recovery is still limited by neuroinflammatory response that resulted from the disruption of blood spinal cord barrier and further damage from secondary injury [2–4]. Therefore, exploring the underlying mechanisms of regulating inflammatory response during SCI should be very useful for developing new therapy strategies.

The first inflammation wave at the initial stage of SCI is caused by activated neutrophil that can migrate to the injury site. Subsequently, tissue resident microglia and lymphocytes as well as monocyte-derived macrophages are recruited, activated and released inflammatory factors, such as tumor necrosis factor-α (TNF-α) and interleukin-1β (IL-1β), leading to the enhanced inflammatory response that further promotes the formation of syringomyelia and glia scar as well as neurological dysfunction [5–7]. Notably, microglia, as issue resident macrophages in the central nervous system, agitates widespread inflammatory response at the different phase of SCI. In the acute phase, microglia polarized to the classically activated microglia (M1) secreting the high level of inducible nitric oxide synthase (iNOS) and pro-inflammatory mediators, such as TNF-α, IL-1β and interleukin-6 (IL-6) to promote inflammatory response and tissue disruption. In the chronic phase, alternatively activated microglia (M2) express the high level of arginase1 (Arg1), mannose receptor (MR, CD206), and other growth factors including transforming growth factor-β (TGF-β) and insulin-like factor1 (IGF1), to halt excessive inflammatory responses and promote the repair of the injured spinal cord [8, 9]. Thereby, targeting

Li *et al. Journal of Translational Medicine*   (2024) 22:724

Page 3 of 16

different polarized microglia should be a new strategy for SCI therapy. Recently, many efforts have been made to attenuate inflammation after SCI by blocking different microglia activity [8]. Noteworthy, Kobashi et al. report that transplantation of interleukin-4 (IL-4) induced M2 microglia can promote recovery of motor function in murine SCI model [10], suggesting that cell therapy with optimized microglial phenotype might be a potential avenue for SCI treatment. However, our and other's studies have shown that M2 polarized macrophages easily switch their phenotype with the various stimuli under pathological microenvironment [11–13]. Therefore, to memory the status of transplanted M2 microglia for effective SCI therapy needs to be further investigated.

Many studies have reported that miRNAs regulate M1/M2 macrophage/microglia polarization and maintain their polarization state [14, 15]. microRNAs (miRNAs) are ~ 22 nt small endogenous noncoding RNAs that induce the decay of mRNA and translational suppression through the interaction with the complementary sequences in the 3'-untranslated region (3'-UTR) of target gene [16]. In order to find the potential miRNA candidates for memorizing M2 polarized status, we took advantage of miRNAs database combined with the literatures [17, 18], and screened out miR-145a-5p as a key miRNA on regulating M2 macrophage polarization [19–21]. After that, microglia were transfected with miR-145a-5p followed with the LPS+IFN-γ or IL-4 stimulation, the results showed that miR-145a-5p indeed promoted M2 while inhibited M1 microglia polarization. Accordingly, miR-145a-5p modified M2 microglia were administrated into the SCI mice, and a series of experiments were performed and demonstrated that transplantation of miR-145a-5p overexpressed M2 microglia could enhance the injured spinal cord recovery and reduce neuron damage by suppressing inflammatory response through targeting TLR4/NF-κB signaling.

Materials and methods
Mice
Animal experiments were conducted with male mice on C57BL/6 background (18–20 g, 6-8wks). In some case CX3CR1^{GFP} transgenic mice (stock#005582, Jackson Laboratory, Bar Harbor, ME, USA) were used for tracing CX3CR1$^+$ microglia. All mice were housed under specific pathogen-free (SPF) conditions, and maintained in separate cages on a 12/12hr light/dark cycle at 21 ± 2 °C and 50% relative humidly as well as were free access to food and water at all time. The mouse genotype was detected by PCR with genomic DNA extracted from mouse tail. All primers were listed in Table S1.

All animal experiments were approved by the Animal Experiment Administration Committee of Fourth Military Medical University. All animal manipulations were performed in accordance with the National Institutes of Health Guide for the Care and Use of Laboratory Animals (NIH Publications, eighth edition) revised in 2012, and all efforts were made to minimize animal numbers and their sufferings.

Primary microglia isolation and cell culture
In order to analyze the contribution of tissue-resident macrophages during SCI, primary microglia were isolated according to the reported method with a little modification [22]. The neonatal mice were immersed into 75% alcohol for 5 min in order to disinfect fully, and then were decapitated. The skull and meningeal were cut out from their brains with ophthalmic scissors and tweezers, and the cerebral cortex was diced up using a flamed razor blade to ensure no tissue chunks remained. To add trypsin-EDTA solution (0.25%:0.02%, C0201, Beyotime, China) into the shredded tissue and incubate them in the 37℃ incubators for 20 min for complete digestion. Then, the cells were seeded into a 75 cm flask, and cultured with Dulbecco's modified Eagle's medium (DMEM, 11965092, Gibco, USA) containing 10% fetal bovine serum (FBS) and 2 mmol/L L-glutamine, supplemented with 10% penicillin-streptomycin (C0222, Beyotime, China) and 20 ng/mL Macrophage Colony Stimulating Factor (M-CSF) in a 5% CO_2 incubator at 37℃. After 14 days, the mixed cells were separated at 200 rpm for 4 h and the microglia were cultured in cell plate overnight.

Microglia polarization and cell transfection
Primary microglia and BV2 cells (microglia cell line) were cultured in DMEM with 10% FBS plus 2 mmol/L L-glutamine, respectively. Primary microglia or BV2 cells were stimulated with LPS (50 ng/mL, Sigma, St. Louis, MO, USA) and IFN-γ (20 ng/mL, PeproTech, Rocky Hill, USA) or IL-4 (20 ng/mL, PeproTech) for 24 h to induce M1 or M2 polarized microglia. Cells were transfected with synthetic miR-145a-5p mimics or antisense oligonucleotides (ASO) (RiboBio Biotech, Guangzhou, China), and siRNA against TLR4 or control oligoribonucleotides (Ctrl) using Lipofectamine 2000(Invitrogen, USA), respectively. The sequences of miR-145a-5p and siRNA against TLR4 were shown in Table S1.

Reporter assay
The 3'-UTR of TLR4 was amplified using a mouse cDNA library as a template, and point mutations were also generated by PCR. The PCR primers were listed in Table S1. Wild-type or mutant 3'-UTR fragments of TLR4 were inserted into the pGL3-promoter (Promega, Madison, WI, USA) to generate reporter plasmids. HEK293T cells were seeded to 48-well plates overnight, and then transfected with different combinations containing reporter plasmids and miRNA using Lipofectamine 2000 reagent,

with a Renilla luciferase vector (phRL-TK, Promega) as an internal control. Cells were harvested 24–48 h after transfection, and the relative luciferase activity was measured with the Dual Luciferase Reporter Assay System (Promega, Madison, WI, USA).

In vivo cell therapy for SCI mice

Mice were anesthetized with sodium pentobarbital (80 mg/kg, intraperitoneally). Then, the hair was removed from their dorsal and the surrounding skin was disinfected with 70% ethanol. Bilateral laminectomy of vertebrae T9 was performed to expose the spinal cord without damaging the dura. The clip compression model was adopted to induce spinal cord injury (SCI) using modified Domont type forceps as described previously [23]. The spinal cord was compressed laterally and vertically from both sides for 30 s using a pair of forceps with a tip width of 0.3 mm on mice. All operations were carried out under microscope.

Mice were mounted on a stereotaxic apparatus. The M2 microglia with oligoribonucleotides (oligo) or miR-145a-5p overexpressed M2 microglia were diluted to a concentration of $9 \times 10^5/30$ μL. Then 5μL of Matrigel (Corning, New York, NY, USA) with miR-145a-5p overexpressed M2, M2 microglia with oligo ($1.5 \times 10^5/5$ μL) or 5 μL Matrigel was injected into the center of the injured spinal cord slowly and vertically using a Hamilton syringe, respectively. Mice suffering laminectomy alone served as sham group. All operations were carried out under microscope.

All the surgeries were performed under aseptic conditions. Animal care was conducted under the Guide for Use of Experimental Animals of Fourth Military Medical University. After confirmation of Matrigel solidification, the spine and subcutaneous tissues were manually restored. Put the food and water in a place where mice can contact convincedly, and massage the bladder of mice gently to help them urinate twice a day.

Behavior analysis

After cell therapy, locomotive function was evaluated by the Basso Mouse Scale (BMS) [24], the hindlimb reflex score [10] and the Louisville Swim Scale (LSS) [25] according to the literature described. For BMS, mice were placed in an open field and observed for over 4 min using a 0-9-point rating system. For hindlimb reflex score, mice were suspended by the tail at a height of 30 cm for 14 s, and then posture was scored according to the following criteria: 0, normal; 1, failure to stretch hindlimbs; 2, hindlimb clasping; and 3, hindlimb paralysis. For LSS, to evaluate three characteristics of swimming that are highly altered by spinal cord injury–namely, hindlimb movement, forelimb dependency, and body position. The motor function was quantified before SCI and on the 1st,

3rd, 5th, 7th, 10th, 12th, 14th, 21th, and 28th days post-injury (dpi). All behavioral analyses were carried out by two observers blind with respect to the identity of the animals.

Immunohistochemistry staining

For the histology and immunofluorescence experiments, mice were anesthetized with sodium pentobarbital(80 mg/kg) via intraperitoneal administration, the then were transcardially perfused with sterile 0.9% normal saline followed by 4% PFA in PBS (pH 7.4). Spinal cords of T9 level (5 mm above and below around the lesion epicenter) were dissected out and then were immersed in PBS solution containing 30% sucrose at a 4℃ freezer for 2 days. For each mouse, a spinal cord segment of 5 mm centered over the lesion site was embedded in optimal cutting temperature (OCT) compound, 14 μm-thick longitudinal frozen sections were cut continuously with a microtone (Leica Biosystems Ltd, shanghai), and then performed by immunofluorescence staining. Some mice were fixed for 3 h (without dehydration). The spinal cord segment of 10 mm centered over the lesion site was made and 5 μm consecutive tissue sections was cut in longitudinal direction with the microtome followed by immunohistochemistry staining. The tissue sections were finally observed with a laser confocal microscope (FV-100, Olympus, Tokyo). The antibody information was listed in Table S2.

Histopathological staining

At 28 dpi, paraffin sections from each group were heated at 60 °C, placed in xylene I and II for 30 min, and then placed in gradient alcohol solutions of 100%, 100%, 95%, 95%, and 80% for 5 min each. The sections were rinsed twice with double-distilled water, and continued with the following experiments.

Hematoxylin and eosin (HE) staining was carried out as previously described [26]. Briefly, sections were incubated with hematoxylin for 1 min, double-rinsed in distilled water, and differentiated in 1% hydrochloric acid, following double-rinsed in distilled water, and then stained with eosin (Sigma-Aldrich) for 2 min.

For Nissl staining, tissue sections were incubated in 0.1% cresyl-violet acetate (Sigma-Aldrich; Merck KGaA) at room temperature for 10 min. The tissues were rinsed in double-distilled water for 8 min and differentiated in 70% ethanol with acetic acid for 2 min.

For Luxol fast blue (LFB) staining, tissue sections were incubated in 0.1% LFB (Sigma, St. Louis, MO, USA) in acidified 95% ethanol overnight at 60 °C. The slides were then differentiated and counterstained with 0.05% lithium carbonate aqueous solution for 10s and then put in a 70% alcohol solution for 20s.

All sections were dehydrated by a conventional alcohol gradient (80%, 95%, 95%, 100%, 100% alcohol for 2 min), placed in xylene I and II for 10 min, and then sealed with neutral gum. Finally, these tissue sections were observed under a microscope, and photographed with an image acquisition system. Three blinded experimenters calculated and quantitatively analyzed the cell number of infiltration and surviving neurons, and the lesion area of myelin using Image-Pro Plus 6.0 (Media Cybernetics Inc., USA). For each mouse, five spinal cross-sections in the rostral-caudal plane taken from the level of the injury were analyzed.

qRT-PCR
Total RNA extraction, reverse transcription, and real-time PCR were performed as described previously [27], with β-actin or U6 RNA (for miRNA) as internal control. The PCR primers are shown in Table S1.

Western blot
Total cells were lysed in the RIPA buffer supplemented with protease inhibitors (Beyotime, Shanghai, China). Protein concentration was determined with a BCA Protein Assay Kit (Pierce, Waltham, MA, USA). Samples were separated by SDS-PAGE, and blotted on polyvinylidenefluoride (PVDF) membranes. Membranes were blocked with 5% skim milk solution for 2 h and probed with primary and secondary antibody, as listed in Table S2. Membranes were developed using chemoluminescent reagents (Pierce).

TUNEL assay and flow cytometry
Apoptotic cells were detected using TUNEL assay kit (Promega, Madison, WI) according to the supplier's instructions. Single cell suspensions of injured spinal cord were prepared by previously described [28], and then cells incubated with primary antibodies and secondary antibodies listed in Table S2, dead cells were excluded by 7-AAD staining, and then analyzed using FACS CantoII (BD Biosciences, San Jose, CA). Data were analyzed using Flowjo V.10 software (TreeStar, Ashland, OR).

Statistics
All values are presented as the means±SD or SEM. Statistical differences between two groups were analyzed using an unpaired t-test. Multigroup differences were assessed by one-way analysis of variance (ANOVA) followed by Tukey's post hoc test. The behavioral score was analyzed using two-way ANOVA with Bonferroni post hoc tests. Images were quantitatively analyzed using Image Pro Plus 6.0 software (Media Cybernetics Inc., USA). Graph Pad Prism 8.4.2 software was used to carry out the statistical analyses. $P < 0.05$ was considered as a statistically significant difference.

Results

At the acute phase of SCI, tissue resident microglia were dominant macrophage population on the lesion sites
Because vigorous inflammatory reaction occurs during the acute phase of SCI, to analyze the dynamic change of inflammatory cells become more meaningful for SCI therapy. Herein, we established a standard spinal cord clamp contusion mouse model to mimic clinical SCI [23], and then analyzed the immune cell subsets of injured spinal cord at different time points using FACS (Figure S1A-D). The results showed that the percentage of Ly6G$^+$ granulocytes increased dramatically at 24 h after SCI, and then decreased gradually to the steady-state level post-SCI 7days (7dpi) (Figure S1E). Simultaneously, CD11b$^+$ myeloid cells presented a continuous ascension and reached to the peak after day 3 of SCI (3dpi) as well as maintained a relative high level on 7dpi (Figure S1F). Further comparative analysis showed that the percentage of CD11b$^+$CD45^{lo} (microglia) was more dominant macrophage subsets at the different time points of SCI compared with the CD11b$^+$CD45^{hi} monocyte-derived macrophages (Figure S1G, H), indicating that microglia could contribute more to SCI during the acute phase. Targeting the microglia should be one alternative strategy to treat SCI.

miR-145a-5p was highly expressed in M2 type microglia, and overexpression of miR-145a-5p promoted M2 while inhibited M1 microglia polarization
Recently, Kobashi et al. report that transplantation of M2-deviated microglia promotes recovery of motor function after SCI [10]. However, because M2 macrophages are unstable and easily change their phenotype in tissue microenvironment [11, 29, 30], therefore, it is better to memory the identity of transplanted M2 microglia in vivo. Our previous studies have reported that microRNAs can regulate macrophage polarization as well as memory the polarized macrophage status [11, 31, 32], we wondered whether there is specific microRNA to memory M2 microglia status. Fortunately, miR-145a-5p, one microRNA exclusively related with M2 macrophages [17, 18], was highly expressed in M2 polarized microglia (Figure S2A). Next, to better understand the role of miR-145a-5p during microglia polarization, we transfected miR-145a-5p mimics or NC into microglia cell line BV2 cells followed with the PBS, LPS+IFN-γ or IL-4 stimulation for 24 h. Both qRT-PCR and Western blot showed that transfection with miR-145a-5p mimics in microglia markedly promoted the expression of M2 related markers including Arg1, Mrc1, YM1 and IL-10, while inhibited the level of M1 markers, such as TNF-α, IL-6, IL-1β and iNOS (Fig. 1A, C and D). As expected, this effect was completely reversed after miR-145a-5p antisense oligonucleotides (ASO) transfection (Fig. 1B, E and F).
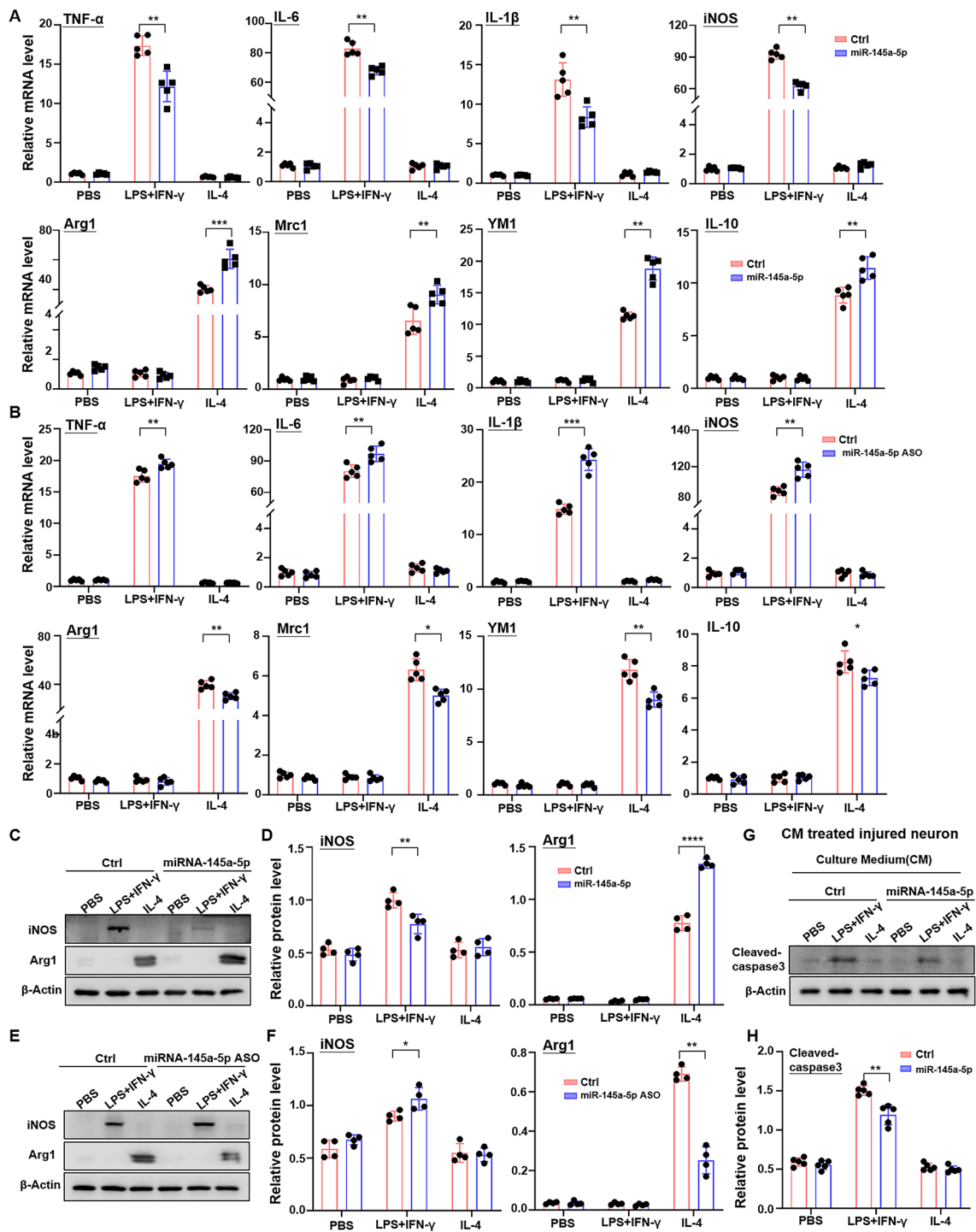
Fig. 1 miR-145a-5p promoted M2 while inhibited M1 microglia polarization leading to the reduced oxidative stress-induced neuron damage. (**A**) BV2 cells were transfected with miR-145a-5p mimics or Ctrl and stimulated with PBS, LPS + IFN-γ or IL-4 for 24 h, respectively. The mRNA level of M1 markers including TNF-α, IL-6, IL-1β and iNOS, as well as M2 markers containing Arg1, Mrc1, YM1 and IL-10 were determined by qRT-PCR, respectively (*n* = 5). (**B**) BV2 cells were transfected with miR-145a-5p ASO or Ctrl and treated as (**A**). The mRNA level of M1 and M2 markers were determined by qRT-PCR, respectively (*n* = 5). (**C**, **D**) BV2 cells were treated as (**A**), and then collected and lysed. The protein level of iNOS and Arg1 were detected by Western blot. Representative image (**C**) and quantitative data (**D**) were shown (*n* = 4). (**E**, **F**) BV2 were treated as (**B**), and then collected and lysed. The protein level of iNOS and Arg1 were detected by Western blot. Representative image (**E**) and quantitative data (**F**) were shown (*n* = 4). (**G**, **H**) The supernatant of BV2 cells treated as (**A**) was collected, and then co-cultured with H_2O_2-treated hippocampal neurons. The activated cleaved-caspase 3 of neuron was determined by Western blot. Representative image (**G**) and quantitative data (**H**) were shown (*n* = 4). Data shown as mean ± SEM. *, *p* < 0.05; **, *p* < 0.01; ***, *p* < 0.001; ****, *p* < 0.0001 by unpaired student's t-test. ASO, antisense oligonucleotides
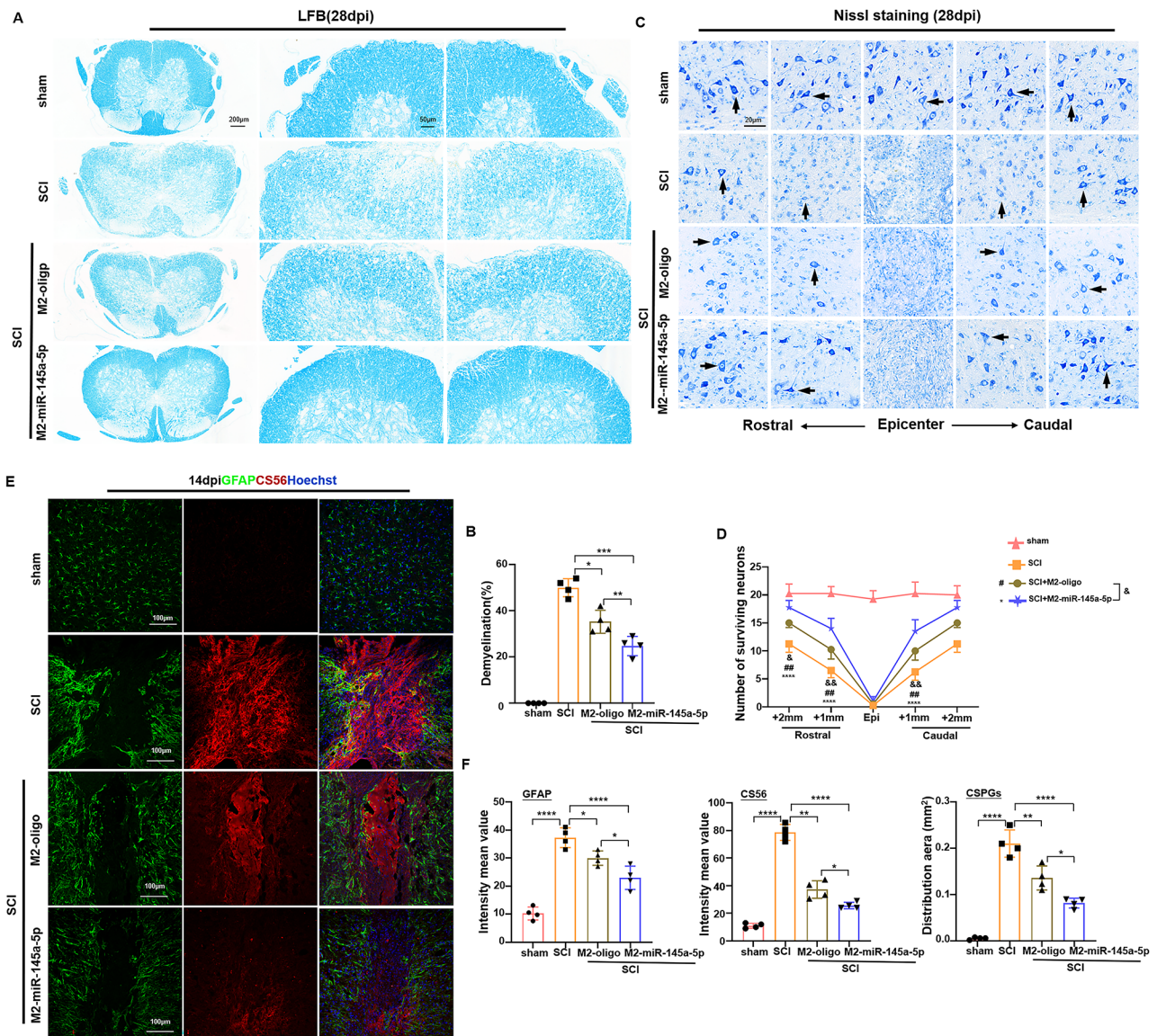
Fig. 2 Injured spinal cord was obviously repaired after transplantation miR-145a-5p overexpressed M2 microglia. (**A**) Representative images of Luxol Fast Blue (LFB) staining with coronal spinal cord sections after cell transplantation 28 days. Scale bars = 200 μm. (**B**) Quantitative analysis of the demyelination in SCI tissue sections with different treatment shown in (**A**) ($n = 4$). (**C**) Representative images of Nissl's staining in SCI tissue sections with different treatment 28 days. Scale bars = 20 μm. (**D**) Quantitative analysis of the number of survival neurons at different distance from the epicenter of injury in each group shown in (**C**) ($n = 4$). (**E**) Representative images of immunofluorescent analysis of CS56 (red), GFAP (green) and Hoechst (blue) on injured spinal cord tissue sections with different treatment 2 weeks. Scale bars = 100 μm. (**F**) Quantitative analysis of mean intensity value of CS56 and GFAP as well as the CSPGs+ area in different group shown in (**E**) ($n = 4$). Data shown as mean ± SEM. *, $p < 0.05$; **, $p < 0.01$; ***, $p < 0.001$; ****$p < 0.0001$ by one-way ANOVA with Turkey's multiple comparison test

These results were further confirmed using cultured different polarized CX3CR1+ primary microglia after miR-145a-5p transfection (Figure S2B-2 J).

Moreover, in order to assess whether miR-145a-5p overexpressed microglia can exert the protective effects on injured neuron in vitro, we treated primary hippocampal neurons with 100μM H_2O_2 for 0.5 h to induce the oxidative stress-induced neuron damage according to the previous studies [33–35]. And then, to incubate them with the conditional medium (CM) from cultured different polarized microglia with or without miR-145a-5p overexpression. After co-culture 6 h, cells were lysed and cleaved-caspase3 were detected. The results showed that miR-145a-5p-transfected M1 microglia could significantly decrease the expression of activated caspase3 in neuron than M1 microglia alone (Fig. 1G, H). Consistently, the number of TUNEL+ apoptotic neurons were also remarkably reduced after co-cultured with the CM

from the miR-145a-5p-transfected M1 microglia (Figure S2K, L). Taken together, these results indicated that the overexpression of miR-145a-5p in microglia could promote M2 while repress M1 microglia polarization, leading to the neuron injury and apoptosis reduction.

Transplantation of miR-145a-5p-overexpressed M2 microglia promoted tissue repair of murine SCI

Next, we expected to investigate whether delivery of miR-145a-5p-overexpressed M2 microglia were more benefit for SCI recovery than M2 microglia transfected with oligoribonucleotides (M2+oligo) transplantation. Firstly, we harvested the primary microglia from the cerebral cortex of neonatal C57BL/6 mice on the first day of birth according to the reported protocol [22]. And then, determined the purity of isolated primary microglia by FACS. As the Figure S3A shown, the percentage of $CD45^+CD11b^+$ microglia could reach to 98.7%. Secondly, we cultured miR-145a-5p overexpressed microglia followed with IL-4 stimulation, as well as established murine SCI model according to the previous study (Figure S3B-D). Continuously, we examined the cell transplantation efficiency by injecting the Cy5 labeled miR-145a-5p microglia into the lesion site of spinal cord, and found that a large amount of $Cy5^+$ cells appeared in the injured spinal cord area (Figure S4A). Accordingly, we delivered the M2 microglia or miR-145a-5p-transfected M2 microglia (namely M2-miR-145a-5p) to the injured site of spinal cord and performed further experiments as shown in the scheme of Supplemental Fig. 3E.

To evaluate the therapy effects of M2-miR-145a-5p microglia administration on SCI mice, spinal cord sections after cell administration 28 days were stained by Hematoxylin and Eosin (HE) staining and Luxol Fast Blue (LFB) staining. Compared to the SCI group and SCI treated with M2 microglia (SCI+M2) group, SCI treated with M2-miR-145a-5p microglia (SCI+M2-miR-145a-5p) group showed the obvious narrowed wound area of spinal cord (Figure S4B, C). Consistently, LFB staining of coronal sections showed the least demyelination area in SCI+M2-miR-145a-5p group (Fig. 2A, B). Moreover, Nissl staining for ventral motor neurons exhibited more survived neuron at injury site except epicenter area in SCI+M2-miR-145a-5p group compared to the other groups (Fig. 2C, D). In addition, using immunofluorescent staining with the longitudinal injured spinal cord sections, the expression of glial fibrillary acidic protein (GFAP) and chondroitin sulfate proteoglycan (CSPG) that are the astrocytes markers displayed significant reduction after M2-miR-145a-5p microglia treatment 2 weeks, although M2 microglia treatment also showed less density of astrocytes in the lesion site (Fig. 2E, F). Collectively, these results demonstrated that M2-miR-145a-5p microglia transplantation could be more benefit for tissue repair of injured spinal cord compared to the M2 microglia treatment.

Transplantation of miR-145a-5p-overexpressed M2 microglia enhanced the locomotor recovery of SCI mice

We further investigated the recovery of locomotive function of SCI mice after transplantation of M2-miR-145a-5p microglia using the Basso mouse scale (BMS), BMS subscore, the Louisville Swimming Scale (LSS) and hindlimb reflex scoring. BMS and BMS subscore indicated that the motor function of SCI mice gradually recovered in all treatment groups. However, the locomotive function recovery was significantly faster in the M2-miR-145a-5p microglia group than that in the M2 microglia group at each time points after cell transplantation (Fig. 3A-C). Similarly, LSS score, which was calculated depending on hindlimb movement, forelimb dependency and trunk instability as well as the body position, indicated that M2-miR-145a-5p microglia treatment could remarkably improve the movement ability of SCI mice compared with the other treatment group (Fig. 3D, E). Similarly, for hindlimb reflex scoring, a significant improvement was also observed after transplantation of the M2-miR-145a-5p microglia into SCI mice 28 days (Fig. 3F). In a word, transplantation of miR-145a-5p-overexpressed M2 microglia improved the locomotive function of SCI mice, even better than M2 microglia transplantation.

Transplantation of miR-145a-5p-overexpressed M2 microglia alleviated inflammatory reaction in murine SCI model by enhancing M2 macrophage phenotype

Next, we wondered whether tissue repair of injured spinal cord after M2-miR-145a-5p microglia transplantation was due to the increased anti-inflammation M2 microglia. In order to address this question, we observed the phenotype of tissue-resident $CX3CR1^+$ microglia using Arg1 immunofluorescence staining on the 3rd, 7th, and 28th day after cell transplantation. The results showed that the expression of Arg1 in $CX3CR1^+$ microglia was significantly higher in the M2-miR-145a-5p group than that in M2 microglia group (Fig. 4A-E). Furthermore, the protein level of M1 and M2 markers were detected by Western blot after cell transplantation 7 days. As expected, the expression of Arg1 was also higher in M2-miR-145a-5p group than that in M2 transplanted group, whereas the expression of iNOS and TNF-α was decreased significantly in M2-miR-145a-5p group (Fig. 4G, H). Consistently, infiltrated inflammatory cells in injured spinal cord were less in M2-miR-145a-5p group than those in M2 and control group by HE staining (Fig. 4I, J). Collectively, these results indicated that transplantation with M2-miR-145a-5p microglia could enhance the M2 microglia polarization in the injured
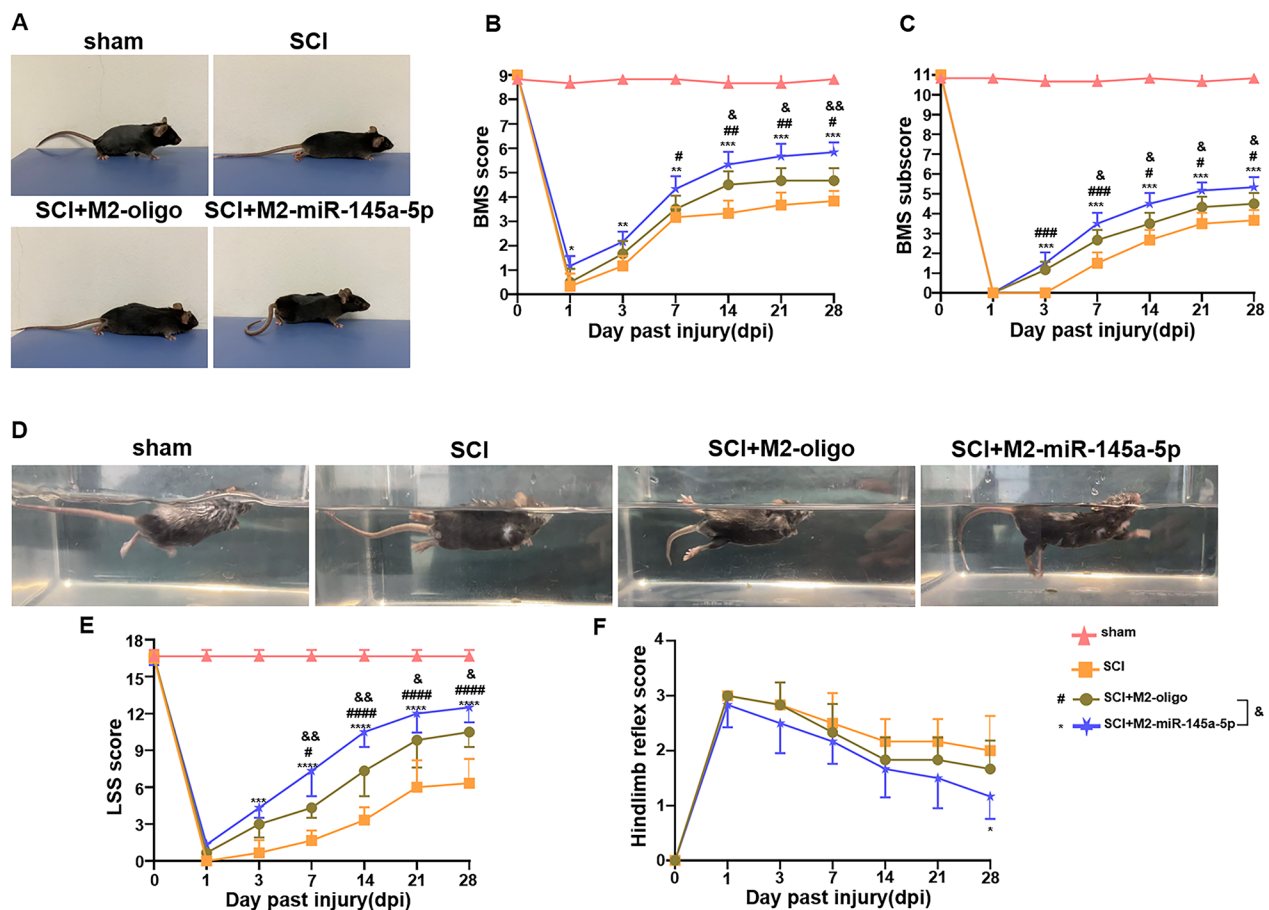
Fig. 3 miR-145a-5p overexpressed M2 microglia transplantation improved the locomotor function of SCI mice. (**A**) Mouse movement behaviors on a plank were photographed in different group including sham, SCI, SCI with M2+oligo microglia delivery, and SCI with miR-145a-5p overexpressed M2 microglia delivery after 28 days. (**B**, **C**) The Basso mouse scale (BMS) score (**B**) and subscore (**C**) in (**A**) were analyzed and quantitatively compared ($n=6$). (**D**) Mouse swimming in water in different group was recorded. (**E**) LSS score in (**D**) was statistically analyzed ($n=6$). (**F**) hindlimb reflex scoring was statistically analyzed ($n=6$). Data shown as mean ± SEM, *, $p<0.05$; **, $p<0.01$; ***, $p<0.001$; ****, $p<0.0001$, SCI mice with M2-miR-145a-5p microglia treatment versus SCI mice without treatment. #, $p<0.05$; ##, $p<0.01$; ###, $p<0.001$; ####, $p<0.0001$, SCI mice with M2 microglia treatment versus SCI mice without treatment. &, $p<0.05$; &&, $p<0.01$; &&&, $p<0.001$; &&&&, $p<0.0001$, SCI mice with M2-miR-145a-5p microglia treatment versus SCI mice with M2 microglia treatment. Statistical analysis was performed using a two-way repeated ANOVA with Bonferroni's post hoc test

area of spinal cord as well as reduce inflammatory reaction of SCI mice.

miR-145a-5p suppressed inflammation by targeting the TLR4/NF-κB signaling in vitro

Based on observation above, we further expected to uncover the mechanisms of miR-145a-5p in M2 microglia benefited the tissue repair of SCI. Taking advantage of miRNA target gene prediction databases in miR-Walk, we predicted and screened out TLR4 as potential target gene of miR-145a-5p. The binding sequence of miR-145a-5p on 3'-UTR of TLR4 as shown in Fig. 5A. And then, the reporter assay showed that overexpression of miR-145a-5p in microglia cell line BV2 definitely reduced luciferase activity of cells transfected with reporter plasmids containing the wild-type 3'-UTR of TLR4, whereas disruption of the proximal seed sequence

(1737−1744 bp) of TLR4 3'-UTR completely abrogated this effect (Fig. 5B). Subsequently, BV2 cells were transfected with miR-145a-5p mimics or control followed by PBS, LPS+IFN-γ or IL-4 stimulation for 24 h, and the levels of TLR4 and NF-κB signaling related molecules were determined by Western blot (Fig. 5C). The results showed that the expression of TLR4 and the phosphorated p65(P-p65) were significantly decreased in miR-145a-5p overexpressed microglia under different polarized status (Fig. 5D). Moreover, to confirm the contribution of TLR4 to miR-145a-5p-mediated inflammation repression, we co-transfected microglia with a miR-145a-5p inhibitor and siRNA targeting TLR4 followed with LPS+IFN-γ stimulation. The results showed that knockdown of TLR4 indeed reduced the phosphorated level of p65. Meanwhile, the miR-145a-5p inhibitor not only rescued the expression of TLR4/NF-κB pathway
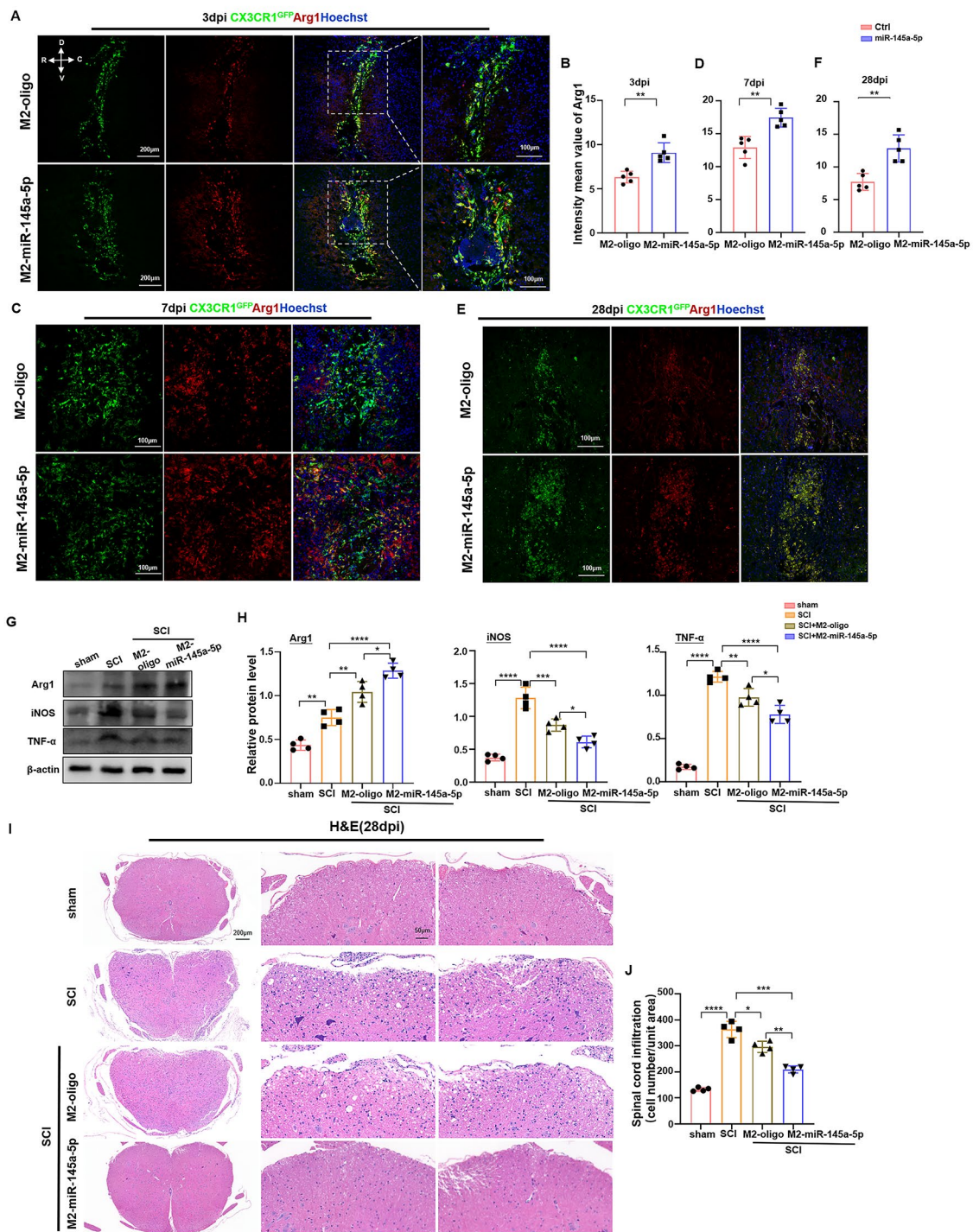
Fig. 4 Delivery of M2 microglia transfected with miR-145a-5p alleviated inflammation in SCI mice. (**A**-**F**) CX3CR1$^{GFP/+}$ microglia were transfected with miR-145a-5p mimics or Ctrl and stimulated with IL-4 to induce M2 microglia, and then to delivery these microglia into SCI mice, respectively. After transplantation 3, 7 and 28 days, Arg1, as an M2 marker, was stained (**A**, **C**, **E**). Nucleic was costained with Hoechst. The mean inflorescence intensity of Arg1$^+$ microglia was measured and quantitatively compared (**B**, **D**, **F**) ($n = 5$). (**G**, **H**) The protein level of the Arg1, iNOS, and TNF-α in injured spinal cord was detected by Western blot after cell transplantation 7 days (**G**). The quantitative data were calculated and shown in (**H**) ($n = 4$). (**I**) Representative images of HE staining with SCI sections after cell treatment 28 days. Scale bars = 200 μm. (**J**) The infiltrated inflammatory cells were counted and quantitatively compared ($n = 4$). Data shown as mean ± SEM. *, $p < 0.05$; **, $p < 0.01$; ***, $p < 0.001$; ****, $p < 0.0001$ by one-way ANOVA with Turkey's multiple comparison test
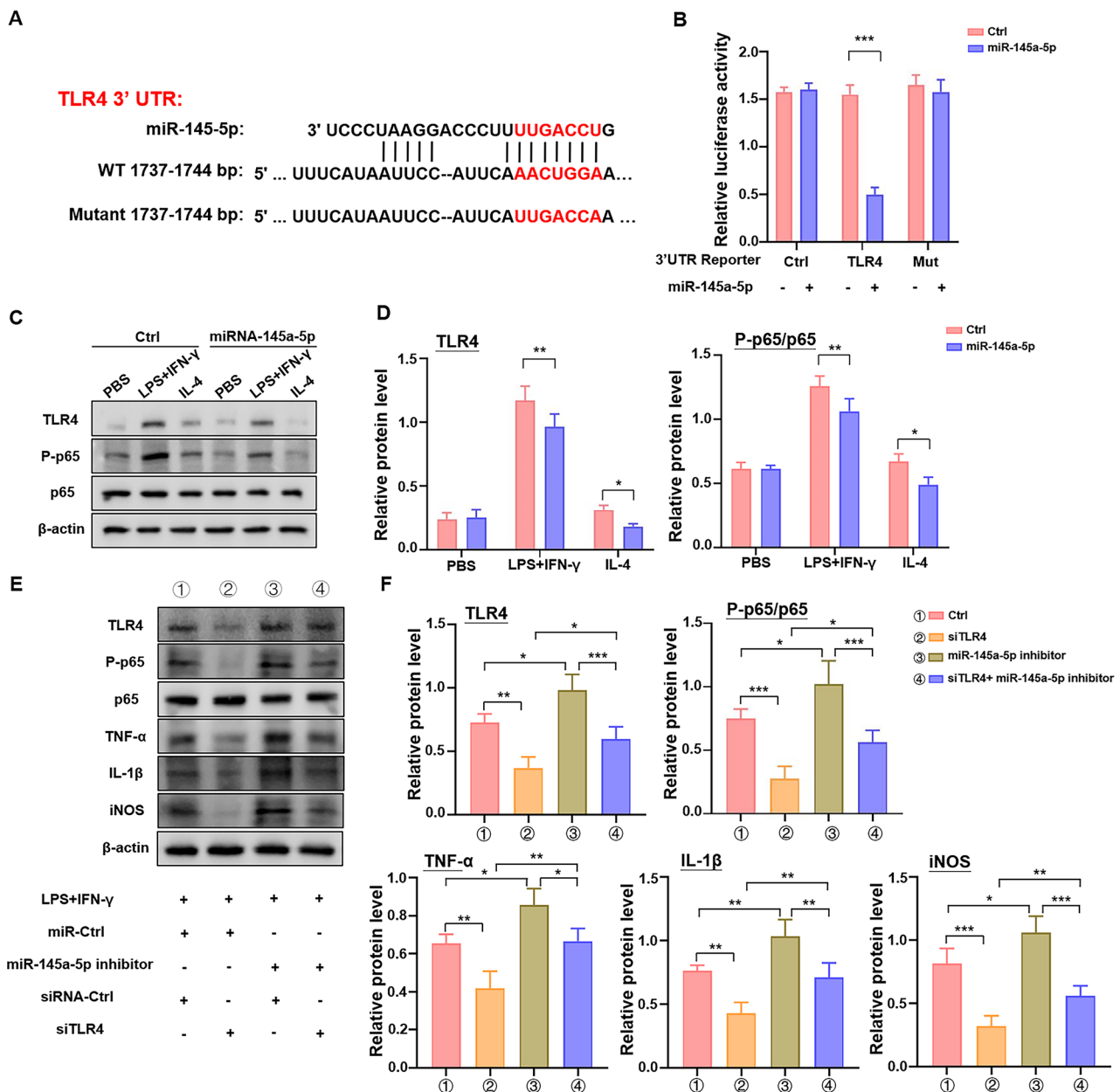
Fig. 5 miR-145a-5p suppressed inflammation by targeting TLR4/ NF-κB signaling in vitro. (**A**) Schematic diagrams showing the predicted binding sequence between miR-145a-5p and wide-type (WT) or mutant 3'-UTRs of TLR4. (**B**) Dual luciferase assay was performed in HEK293T cells after co-transfected with reporter plasmids containing WT or mutant 3'-UTRs of TLR4 as well as miR-145a-5p mimics or Ctrl ($n = 4$). (**C**) Representative Western blot showing the expression of TLR4 and NF-kB signal-related molecules such as p65 in BV2 that were transfected with miR-145a-5p mimics or Ctrl followed by PBS, LPS + IFN-γ or IL-4 stimulation for 24 h. (**D**) Quantitative analysis of the protein level of TLR4 and p65 as well as P-p65 in (**D**) ($n = 4$). (**E**) BV2 was transfected with miR-145a-5p inhibitor or Ctrl and siTLR4 followed by LPS + IFN-γ stimulation for 24 h. The expression of TLR4, p65 and P-p65, as well as TNF-α, IL-1β and iNOS was detected by Western blot ($n = 4$). (**F**) Quantitative analysis of the protein level in (**E**) ($n = 4$). Data shown as mean ± SEM, *, $p < 0.05$; **, $p < 0.01$; ***, $p < 0.001$; ****, $p < 0.0001$ by one-way ANOVA with Turkey's multiple comparison test

related molecules but also upregulated the level of M1 markers TNF-α, IL-1β and iNOS, and TLR4 knockdown reversed the effect of miR-145a-5p inhibitor (Fig. 5E, F). Taken together, these results indicated that miR-145a-5p might alleviate the inflammation response by targeting TLR4/NF-κB signaling in vitro.

Transplantation of miR-145a-5p overexpressed M2 microglia attenuated the inflammation response of SCI mice by repressing TLR4/NF-κB signaling

As described in Figure S3B, we established T9 crushed SCI mice model and transplanted M2-miR-145a-5p microglia, M2 microglia or control mixed with matrigel into the epicenter site of injured spinal cord, respectively.

After 7 days of cell transplantation, spinal cord sections of different treatment group were performed immunofluorescence staining with Ibal1, a microglia special marker, and TLR4. As shown in Fig. 6A and B, TLR4 positive signal in Ibal1^{+} cells were significantly reduced at the lesion site after M2-miR-145a-5p microglia administration compared to the Ctrl and M2 microglia group. Subsequently, protein was extracted from the injured spinal cord, and the TLR4/NF-κB pathway related molecules were detected by Western blot (Fig. 6C). The protein levels of TLR4 and P-p65 were also significantly decreased in M2-miR-145a-5p group compared with that in the other groups (Fig. 6D, E). Collectively, these results further verified that delivery of M2-miR-145a-5p microglia could attenuate SCI by inhibiting TLR/NF-κB signaling in vivo.

In summary, our results firstly revealed that delivery of miR-145a-5p overexpressed M2 microglia could promote the tissue repair of murine SCI than M2 microglia transplantation alone. The underlying mechanisms might be that miR-145a-5p promoted anti-inflammation M2 while suppressed pro-inflammation M1 microglia polarization by targeting TLR/NF-κB signaling (Fig. 6F).

Discussion

Microglia, as the tissue resident macrophages originated from the yolk sac of embryo, has been observed to rapidly mobilize to the lesion site and initiate the inflammatory response during the first week post-SCI. Meanwhile, it is found that M2 microglia is transiently occurred in the injury area at the early stage of SCI, while M1 microglia can exist in the lesion site for a long time [36, 37]. Because M2 microglia possess the ability of anti-inflammation and tissue repair while M1 microglia own pro-inflammation and tissue damage features, several studies have been performed to recover SCI by harnessing the M2 microglia phenotype [38–40]. Especially, Kobashi et al. find that transplantation of IL-4-induced M2 microglia promotes the recovery of motor function as well as reduces neuroinflammatory response after SCI [10]. However, under
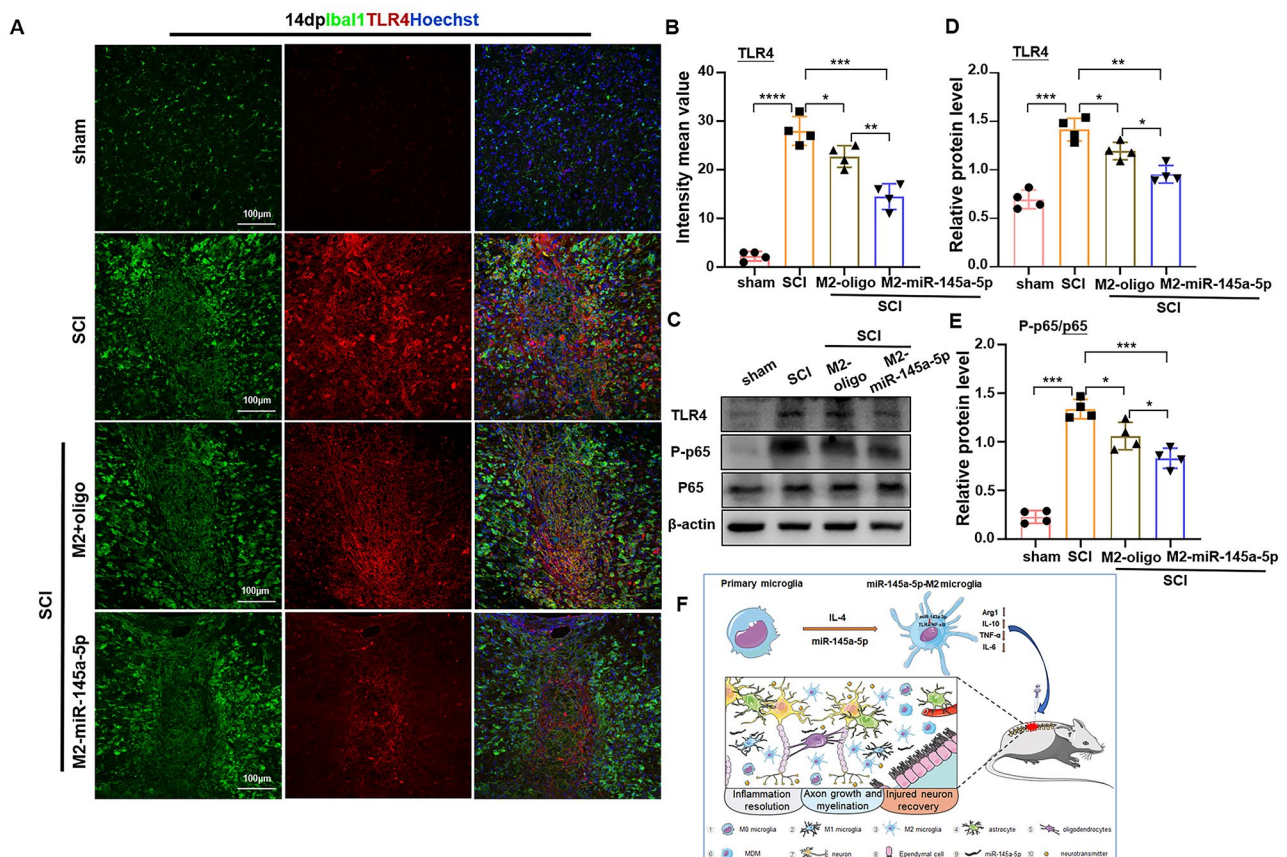

Fig. 6 Transplantation of miR-145a-5p overexpressed M2 microglia attenuated SCI by inhibiting TLR4/NF-κB pathway in vivo. (**A**) Tissue section was stained with Ibal1(Green), TLR4 (Red) and DNA(Hoechst) after different treatment for SCI on day 7. (**B**) Quantitative analysis and comparison of the intensity mean value of TLR4 in (**A**) ($n = 4$). (**C**) The expression of TLR4 and p65 as well as P-p65 were detected by Western blot with the spinal cord lysis from SCI mice with different treatment as (**A**). (**D**, **E**) The protein level of TLR4 (**D**), p65 and P-p65 (**E**) in (**C**) was quantitatively compared ($n = 4$). (**F**) The Scheme of miR-145a-5p overexpressed M2 microglia transplantation promoted the tissue repair of SCI by targeting TLR4/NF-κB signaling and abolishing inflammation response. Data shown as mean ± SEM. *, $p < 0.05$; **, $p < 0.01$; ***, $p < 0.001$; ****, $p < 0.0001$ by one-way ANOVA with Turkey's multiple comparison test

pathological state, M2 macrophages could be more easily re-educated to M1 macrophages, conversely not yet. For example, to impede the tumor progression, many strategies focus on promoting M2-like tumor associated macrophages (TAMs) switch to M1-like TAMs [11, 32]. It is reminiscent of Liu's study in which IL-4-induced M2 microglia exhibit M1 microglia features after secondary LPS stimulation, while LPS-stimulated M1 microglia appear not to respond to a secondary IL-4 stimulation [13]. These studies suggest that complicated mechanisms including epigenetic programs might involve in the regulation of macrophage polarization, and M2 macrophages are easily remodeled by tissue microenvironment. Based on these studies, in current study, to further improve the efficiency of M2 macrophage transplantation for SCI treatment, we took advantage of miRNA modification to memory the M2 phenotype from the epigenetic way, and found that miR-145a-5p, a non-coding RNA molecule, could promote M2 microglia polarization phenotype while inhibit M1 microglia polarization to control inflammatory response. Excitingly, when delivery of miR-145a-5p modified M2 microglia into the injured area, the locomotor function and neuron survival of SCI mice was improved, especially better than M2 microglia transplantation alone. However, in our study, we only observed the SCI recovery after miR-145a-5p modified microglia transplantation 28 days, and its long-term of effect should be studied in the future.

Although surgical decompression and stabilization can treat SCI, the ability of axonal regeneration still is limited. In order to overcome this issue, cell transplantation becomes a more powerful therapy approach to repair the injured spinal cord by replacing damaged and lost resident cells [41, 42]. Currently, a variety of cell types have been tested in SCI treatment, which include multipotent neural stem cells (NSCs), lineage-restricted neural progenitor cells (NPCs), embryonic stem cells (ESCs), mesenchymal stem cells and induced pluripotent stem cells (iPSCs). Despite these cell types are benefit for SCI treatment, several issues including ethical derivation, long-term immunosuppressive agent usage, large amount of homogeneous cell expansion as well as possible carcinogenesis has hindered their clinical application [43, 44]. Considering these issues, autologous immune cells, such as microglia/bone marrow-derived macrophages, have been applied [10, 45]. However, no matter M1 microglia or M2 microglia transplantation, they all show beneficial or detrimental effect. On the one hand, M1 microglia indeed participates in clearance of apoptotic and degenerating myelin. On the other hand, M1 microglia can cause neurological damage via producing some pro-inflammatory factors and proteases. Similarly, M2 microglia one side reduce inflammation response and enhance SCI recovery by expressing anti-inflammatory

factors. Meanwhile, M2 microglia phenotype will be unstable in injured spinal cord microenvironment [38, 46]. Therefore, in this study, we took advantage of epigenetic mechanism to modify M2 type microglia with miR-145a-5p, and found that miR-145a-5p modified M2 microglia definitely promoted the repair of injured spinal cord by attenuating neuroinflammation. What's more, miR-145a-5p overexpressed M2 microglia remained long time in vivo (data not shown), suggesting that M2 microglia features could be stable through epigenetic memory.

microRNAs, as one of epigenetic regulator, play a very important role in cell differentiation, proliferation, apoptosis as well as in disease progress [16, 47, 48]. Using in situ hybridization assay, previous studies have demonstrated that miR-145a-5p is mainly expressed in neural cells, astrocytes and microglia of spinal cord [49]. But, with a contusive SCI model, miR-145a-5p is found to be downregulated in injured spinal cord tissues that is accompanied by massive neurons lost [50, 51]. This result is consistent with our finding that the expression of miR-145a-5p was significantly decreased in mice after SCI 1 day (data not shown). Moreover, the downregulation of miR-145a-5p expression is detected in neurons of murine sciatic nerve injury model that leads to neuron cell death [51, 52]. Similarly, Wang CY et al. has reported that miR-145a-5p is one negative regulator of astrogliosis that can result in the formation of glial barrier and hinder axonal regeneration by targeting GFAP and c-Myc [49]. All these results suggest that miR-145a-5p can exert anti-inflammation role in central nervous system (CNS). Consistently, as an anti-inflammation microRNA, miR-145a-5p mimic also reduce the inflammatory response in airway, vascular smooth muscle and retinal endothelial cells [53–55]. However, we could not ignore the pro-inflammatory role of miR-145a-5p in other pathological situation, such as atherosclerosis [56]. The complicated role of miRNAs might attribute to their different targets and pathway.

The pro-inflammatory immune response driven by activated microglia is a key contributor to the pathogenesis of SCI. The phenotypic transformation of microglia from steady state to the activated state is initiated by some pattern recognition receptors including Toll-like receptor- 4 (TLR4) [57]. Using TLR4-deficient mice combined with the spinal cord ischemia-reperfusion injury model, Bell MT et al. report that TLR4 knockout decrease microglia activation and pro-inflammatory factors production as well as preserve the neuronal viability and motor function of SCI mice [58]. Conversely, TLR4-mediated microglia activation can induce pro-inflammatory cytokines containing TNF-α, IL-6 and IL-1β production by NF-κB signaling, which will aggravate disease progress, such as SCI and several neurodegenerative diseases [59]. These studies indicate that blocking TLR4-mediated inflammation

signaling should be benefit for neuroinflammation abrogation. Interestingly, in our study, TLR4 was identified as one target gene of miR-145a-5p, and overexpressed miR-145a-5p in microglia could remarkably induce M2 type microglia activation while inhibit M1 type by targeting TLR4/NF-κB signaling. Transplantation of miR-145a-5p modified M2 microglia promoted the SCI recovery by reducing neuroinflammation in mice.

Although our work provides another better option with miR-145a-5p modified M2 microglia transplantation for SCI treatment than that with M2 microglia, it still remains some limitations. First, in this study, we used common clip compression SCI murine model that can simulate combined impact-compression in clinic compared with the other models, such as contusion model and transection model etc. Notably, kobashi et al. used the skin biopsy puncher that is uncommon SCI model to observe the effect of M2 macrophage therapy. In future, we may adopt more SCI models to extend our miRNA-modified M2 macrophage application. Second, the mechanisms of miR-145a-5p overexpressed M2 microglia promotes spinal cord injury recovery may need to be further explored. For instance, it is possible that miR-145a-5p overexpressed M2 microglia transplantation promotes SCI recovery by regulating neighboring cells in tissue microenvironment via releasing exosome or the other factors. Except that, because several miRNAs can bind with one target gene to repress mRNA translation, it is possible to combine several same types of miRNAs, which can be transfected into M2 macrophages or encapsulated in nanoparticle for SCI therapy. Last, it is a little far to extend our findings to humans, because human microglia are not easily acquired in vitro, although we can take advantage of iPSCs. In near future whether we can induce microglia from autologous monocytes using gene editing technique is worth of exploring.

In a word, our study firstly demonstrates that delivery of miR-145a-5p overexpressed M2 microglia might promote the locomotor function recovery of SCI mice by targeting TLR4/ NF-κB signaling, the therapy effect of SCI with M2-miR-145a-5p microglia transplantation was better than M2 microglia transplantation.

Abbreviations

SCI	Spinal cord injury
BSCB	Blood-spinal-cord-barrier
TNF-α	Tumour necrosis factor-α
IL-1β	Interleukin-1β
iNOS	Inducible nitric oxide synthase
Arg1	Arginase 1
MR	Mannose receptor
TGF-β	Transforming growth factor-β
IGF1	Insulin-like factor 1
miRNAs	MicroRNAs
3'-UTR	3'-untranslated region
dpi	Day past injury
ASO	Antisense oligonucleotide
CM	Conditional medium
LFB	Luxol Fast Blue
GFAP	Glial fibrillary acidic protein
CSPG	Chondroitin sulfate proteoglycans
BMS	Basso mouse scale
LSS	Louisville swimming scale
NSCs	Neural stem cells
NPCs	Neural progenitor cells
ESCs	Embryonic stem cells
iPSCs	Induced pluripotent stem cells
CNS	Central nervous system
TLR4	Toll-like receptor-4
NF-κB	Nuclear factor-κB

Author contributions

P.L. and J.Z. conducted experiments and analyzed data. Y.M., L.W., S.L. and F.F. helped to perform some experiments including SCI model establishment, microglia isolation and miRNAs detection. T.W. supported FACS assay. L.F. helped to breed mice. X.H. and Y.H. advised on the experimental design and techniques. P.L., Y.H. and H.Q. wrote the manuscript. Z.W. and H.Q. designed the study, analyzed data and revised the manuscript. All authors reviewed the manuscript.

Data availability

Data sharing is not applicable to this article as no datasets were generated or analysed during the current study.

Declarations

Ethics approval and consent to participate

All animal experiments were approved by the Animal Experiment Administration Committee of Fourth Military Medical University. Animal studies were performed in accordance with the Guide for the Care and Use of Laboratory Animals.

Consent for publication

Not applicable.

Conflict of interest

The authors declare that they have no competing interests.

Author details

[1]Department of Orthopedics, Xijing Hospital, Fourth Military Medical University, Xi'an 710032, China
[2]State Key Laboratory of Holistic Integrative Management of Gastrointestinal Cancers, Department of Medical Genetics and Developmental Biology, Fourth Military Medical University, Xi'an 710032, China

References

1. Khorasanizadeh M, Yousefifard M, Eskian M, Lu Y, Chalangari M, Harrop JS, Jazayeri SB, Seyedpour S, Khodaei B, Hosseini M, et al. Neurological recovery following traumatic spinal cord injury: a systematic review and meta-analysis. J Neurosurg Spine. 2019;15:1–17.
2. Wichmann TO, Kasch H, Dyrskog S, Høy K, Møller BK, Krog J, Hviid CVB, Hoffmann HJ, Rasmussen MM. The inflammatory response and blood-spinal cord barrier integrity in traumatic spinal cord injury: a prospective pilot study. Acta Neurochir. 2022;164:3143–53.
3. Hemley SJ, Tu J, Stoodley MA. Role of the blood-spinal cord barrier in post-traumatic syringomyelia. J Neurosurg Spine. 2009;11:696–704.
4. Anjum A, Yazid MD, Fauzi Daud M, Idris J, Ng AMH, Selvi Naicker A, Ismail OHR, Athi Kumar RK, Lokanathan Y. Spinal cord Injury: pathophysiology, Multimolecular interactions, and underlying recovery mechanisms. Int J Mol Sci. 2020;21:7533.
5. Hellenbrand DJ, Quinn CM, Piper ZJ, Morehouse CN, Fixel JA, Hanna AS. Inflammation after spinal cord injury: a review of the critical timeline of signaling cues and cellular infiltration. J Neuroinflamm. 2021;18:284.
6. Milich LM, Ryan CB, Lee JK. The origin, fate, and contribution of macrophages to spinal cord injury pathology. Acta Neuropathol. 2019;137:785–97.
7. Orr MB, Gensel JC. Spinal cord Injury scarring and inflammation: therapies targeting glial and inflammatory responses. Neurotherapeutics: J Am Soc Experimental Neurother. 2018;15:541–53.
8. Brockie S, Hong J, Fehlings MG. The role of Microglia in modulating neuroinflammation after spinal cord Injury. Int J Mol Sci. 2021;22:9706.
9. Li Y, He X, Kawaguchi R, Zhang Y, Wang Q, Monavarfeshani A, Yang Z, Chen B, Shi Z, Meng H, et al. Microglia-organized scar-free spinal cord repair in neonatal mice. Nature. 2020;587:613–8.
10. Kobashi S, Terashima T, Katagi M, Nakae Y, Okano J, Suzuki Y, Urushitani M, Kojima H. Transplantation of M2-Deviated Microglia promotes recovery of motor function after spinal cord Injury in mice. Mol Therapy: J Am Soc Gene Therapy. 2020;28:254–65.
11. Wang L, Hu YY, Zhao JL, Huang F, Liang SQ, Dong L, Chen Y, Yu HC, Bai J, Yang JM et al. Targeted delivery of miR-99b reprograms tumor-associated macrophage phenotype leading to tumor regression. J Immunother Cancer. 2020;8.
12. Dietsche CL, Hirth E, Dittrich PS. Multiplexed analysis of signalling proteins at the single-immune cell level. Lab Chip. 2023;23:362–71.
13. Liu HC, Zheng MH, Du YL, Wang L, Kuang F, Qin HY, Zhang BF, Han H. N9 microglial cells polarized by LPS and IL4 show differential responses to secondary environmental stimuli. Cell Immunol. 2012;278:84–90.
14. Ponomarev ED, Veremeyko T, Weiner HL. MicroRNAs are universal regulators of differentiation, activation, and polarization of microglia and macrophages in normal and diseased CNS. Glia. 2013;61:91–103.
15. Liu G, Abraham E. MicroRNAs in immune response and macrophage polarization. Arterioscler Thromb Vasc Biol. 2013;33:170–7.
16. Lu TX, Rothenberg ME, MicroRNA. J Allergy Clin Immunol. 2018;141:1202–7.
17. Zhang Y, Zhang M, Zhong M, Suo Q, Lv K. Expression profiles of miRNAs in polarized macrophages. Int J Mol Med. 2013;31:797–802.
18. Freilich RW, Woodbury ME, Ikezu T. Integrated expression profiles of mRNA and miRNA in polarized primary murine microglia. PLoS ONE. 2013;8.
19. Yu YL, Yu G, Ding ZY, Li SJ, Fang QZ. Overexpression of mir-145-5p alleviated LPS-induced acute lung injury. J Biol Regul Homeost Agents. 2019;33:1063–72.
20. Chen H, Gao J, Xu Q, Wan D, Zhai W, Deng L, Qie R. MiR-145-5p modulates lipid metabolism and M2 macrophage polarization by targeting PAK7 and regulating β-catenin signaling in hyperlipidemia. Can J Physiol Pharmacol. 2021;99:857–63.
21. Hao Y, Yang L, Liu Y, Ye Y, Wang J, Yu C, Yan H, Xing Y, Jia Z, Hu C et al. Mmu-miR-145a-5p accelerates Diabetic Wound Healing by promoting macrophage polarization toward the M2 phenotype. Front Med. 2021;8.
22. Roy J. Primary microglia isolation from mixed cell cultures of neonatal mouse brain tissue. Brain Res. 2018;1689:21–9.
23. Faulkner JR, Herrmann JE, Woo MJ, Tansey KE, Doan NB, Sofroniew MV. Reactive astrocytes protect tissue and preserve function after spinal cord injury. J Neuroscience: Official J Soc Neurosci. 2004;24:2143–55.
24. Basso DM, Fisher LC, Anderson AJ, Jakeman LB, McTigue DM, Popovich PG. Basso Mouse Scale for locomotion detects differences in recovery after spinal cord injury in five common mouse strains. J Neurotrauma. 2006;23:635–59.
25. Smith RR, Burke DA, Baldini AD, Shum-Siu A, Baltzley R, Bunger M, Magnuson DS. The Louisville swim scale: a novel assessment of hindlimb function following spinal cord injury in adult rats. J Neurotrauma. 2006;23:1654–770.
26. Feldman AT, Wolfe D. Tissue processing and hematoxylin and eosin staining. Methods Mol Biol. 2014;1180:31–43.
27. Singh C, Roy-Chowdhuri S, Quantitative Real-Time PCR. Recent advances. Methods Mol Biol. 2016;1392:161–76.
28. Kabakov AE, Gabai VL. Cell death and survival assays. Methods Mol Biol. 2018;1709:107–27.
29. Orihuela R, McPherson CA, Harry GJ. Microglial M1/M2 polarization and metabolic states. Br J Pharmacol. 2016;173:649–65.
30. David S, Greenhalgh AD, Kroner A. Macrophage and microglial plasticity in the injured spinal cord. Neuroscience. 2015;307:311–8.
31. Huang F, Zhao JL, Wang L, Gao CC, Liang SQ, An DJ, Bai J, Chen Y, Han H, Qin HY. miR-148a-3p mediates Notch Signaling to promote the differentiation and M1 activation of macrophages. Front Immunol. 2017;8:1327.
32. Zhao JL, Ye YC, Gao CC, Wang L, Ren KX, Jiang R, Hu SJ, Liang SQ, Bai J, Liang JL, et al. Notch-mediated lactate metabolism regulates MDSC development through the Hes1/MCT2/c-Jun axis. Cell Rep. 2022;38:110451.
33. Wang H, Liao S, Li H, Chen Y, Yu J. Long non-coding RNA TUG1 sponges Mir-145a-5p to regulate Microglial polarization after oxygen-glucose deprivation. Front Mol Neurosci. 2019;12:215.
34. Yao M, Luo Y, Li H, Liao S, Yu J. LncRNA Tug1 contributes post-stroke NLRP3 inflammasome-dependent pyroptosis via miR-145a-5p/Tlr4 Axis. Mol Neurobiol. 2022;59:6701–12.
35. Tsai YR, Chang CF, Lai JH, Wu JC, Chen YH, Kang SJ, Hoffer BJ, Tweedie D, Luo W, Greig NH et al. Pomalidomide ameliorates H_2O_2-Induced oxidative stress Injury and Cell Death in Rat primary cortical neuronal cultures by inducing anti-oxidative and Anti-apoptosis effects. Int J Mol Sci. 2018;19.
36. Kigerl KA, Gensel JC, Ankeny DP, Alexander JK, Donnelly DJ, Popovich PG. Identification of two distinct macrophage subsets with divergent effects causing either neurotoxicity or regeneration in the injured mouse spinal cord. J Neuroscience: Official J Soc Neurosci. 2009;29:13435–44.
37. Gensel JC, Zhang B. Macrophage activation and its role in repair and pathology after spinal cord injury. Brain Res. 2015;1619:1–11.
38. Chen BY, Zheng MH, Chen Y, Du YL, Sun XL, Zhang X, Duan L, Gao F, Liang L, Qin HY, et al. Myeloid-specific blockade of Notch Signaling by RBP-J knockout attenuates spinal cord Injury accompanied by compromised inflammation response in mice. Mol Neurobiol. 2015;52:1378–90.
39. Xu GY, Xu S, Zhang YX, Yu ZY, Zou F, Ma XS, Xia XL, Zhang WJ, Jiang JY, Song J. Cell-free extracts from Human Fat Tissue with a Hyaluronan-based hydrogel attenuate inflammation in a spinal cord Injury Model through M2 Microglia/Microphage polarization. Small. 2022;18.
40. Kroner A, Greenhalgh AD, Zarruk JG, Passos Dos Santos R, Gaestel M, David S. TNF and increased intracellular iron alter macrophage polarization to a detrimental M1 phenotype in the injured spinal cord. Neuron. 2014;83:1098–116.
41. Assunção Silva RC, Pinto L, Salgado AJ. Cell transplantation and secretome based approaches in spinal cord injury regenerative medicine. Med Res Rev. 2022;42:850–96.
42. Assinck P, Duncan GJ, Hilton BJ, Plemel JR, Tetzlaff W. Cell transplantation therapy for spinal cord injury. Nat Neurosci. 2017;20:637–47.
43. Gabel BC, Curtis EI, Marsala M, Ciacci JD. A review of Stem Cell Therapy for spinal cord Injury: large animal models and the Frontier in humans. World Neurosurg. 2017;98:438–43.
44. Li XC, Zhong CF, Deng GB, Liang RW, Huang CM. Efficacy and safety of bone marrow-derived cell transplantation for spinal cord injury: a systematic review and meta-analysis of clinical trials. Clin Transplant. 2015;29:786–95.
45. Ding Y, Zhang D, Wang S, Zhang X, Yang J. Hematogenous macrophages: a New Therapeutic Target for spinal cord Injury. Front cell Dev Biology. 2021;9:767888.
46. Hu X, Leak RK, Shi Y, Suenaga J, Gao Y, Zheng P, Chen J. Microglial and macrophage polarization—new prospects for brain repair. Nat Reviews Neurol. 2015;11:56–64.
47. Saliminejad K, Khorram Khorshid HR, Soleymani Fard S, Ghaffari SH. An overview of microRNAs: Biology, functions, therapeutics, and analysis methods. J Cell Physiol. 2019;234:5451–65.
48. Bhaskaran M, Mohan M. MicroRNAs: history, biogenesis, and their evolving role in animal development and disease. Vet Pathol. 2014;51:759–74.
49. Wang CY, Yang SH, Tzeng SF. MicroRNA-145 as one negative regulator of astrogliosis. Glia. 2015;63:194–205.
50. Deumens R, Koopmans GC, Joosten EA. Regeneration of descending axon tracts after spinal cord injury. Prog Neurobiol. 2005;77:57–89.
51. Zhang HY, Zheng SJ, Zhao JH, Zhao W, Zheng LF, Zhao D, Li JM, Zhang XF, Chen ZB, Yi XN. MicroRNAs 144, 145, and 214 are down-regulated in primary neurons responding to sciatic nerve transection. Brain Res. 2011;1383:62–70.

52. Guo JB, Chen BL, Song G, Zheng YL, Zhu Y, Yang Z, Su X, Wang Y, Cao Q, Chen PJ, et al. Comparative transcriptome profiling reveals changes of microRNAs response to Exercise in rats with Neuropathic Pain. Neural Plast. 2021;2021:5597139.

53. O'Leary L, Sevinç K, Papazoglou IM, Tildy B, Detillieux K, Halayko AJ, Chung KF, Perry MM. Airway smooth muscle inflammation is regulated by microRNA-145 in COPD. FEBS Lett. 2016;590:1324–34.

54. Guo X, Yu L, Chen M, Wu T, Peng X, Guo R, Zhang B. miR-145 mediated the role of aspirin in resisting VSMCs proliferation and anti-inflammation through CD40. J Translational Med. 2016;14:211.

55. Hui Y, Yin Y. MicroRNA-145 attenuates high glucose-induced oxidative stress and inflammation in retinal endothelial cells through regulating TLR4/NF-κB signaling. Life Sci. 2018;207:212–8.

56. Li S, Sun W, Zheng H, Tian F. Microrna-145 accelerates the inflammatory reaction through activation of NF-κB signaling in atherosclerosis cells and mice. Biomedecine Pharmacotherapie. 2018;103:851–7.

57. Rodríguez-Gómez JA, Kavanagh E, Engskog-Vlachos P, Engskog MKR, Herrera AJ, Espinosa-Oliva AM, Joseph B, Hajji N, Venero JL, Burguillos MA. Microglia: agents of the CNS pro-inflammatory response. Cells. 2020;9.

58. Bell MT, Puskas F, Agoston VA, Cleveland JC Jr., Freeman KA, Gamboni F, Herson PS, Meng X, Smith PD, Weyant MJ, et al. Toll-like receptor 4-dependent microglial activation mediates spinal cord ischemia-reperfusion injury. Circulation. 2013;128:S152–6.

59. Heidari A, Yazdanpanah N, Rezaei N. The role of toll-like receptors and neuro-inflammation in Parkinson's disease. J Neuroinflamm. 2022;19:135.

Publisher's Note